

RFID-automated Smart Air-cargo Movement System

Xin Su* *Regular Member*, KwangHyun Jeon* *Associate Member*, KyungHi Chang*^o *Lifelong Member*

ABSTRACT

This paper aims to build up a RFID-automated cargo movement system in an air-cargo warehouse. In our research, we do the spectrum measurements compliant with the RFID frequency bands to observe the interferences from legacy systems in the air-cargo warehouse. To overcome the dense-reader mode (DRM) problem, we apply three novel approaches, which are the periodic transmit of a reader, the Visible RFID reader & tag, and the sensor-based RFID system. Moreover, for the tag collision issue, we implement the Adaptive Adjustable Framed Q (AAFQ) algorithm, and the demonstration on RFID tag anti-collision algorithms show that the AAFQ algorithm has highly desirable tag anti-collision performance compared to any other commercially available solutions.

Key Words : RFID, Air-cargo, Interference, DRM, Anti-collision, Visible RFID

I. Introduction

Radio frequency identification (RFID) technology^[1,2] has become a viable technology for identifying objects automatically. A RFID system comprises readers (interrogators) and tags (labels). A reader can identify a tag by its unique ID number and obtain the information stored on the tag. In this paper, we aim to develop an RFID assisted air-cargo life-cycle management system which monitors and tracks the air-cargo during the cargo export process. The system works in the air-cargo export flow by using automatic ID identification technology, which can automate the air-cargo export process. Thus, it can not only shorten the system turn-around time but also optimize the resources management. This technologies proposed can be applied to air-cargo import process also.

We have primarily completed three major tasks in this research. We measure radio interferences in our target warehouse first. Though the interferences from legacy systems are negligible, we face the problems of dense-reader mode (DRM) and tags

collision according to the scenarios of the cargo movement process.^[3-9] We suggest multiple solutions to overcome the problem for each analyzed scenario, and then the proposed solutions are evaluated with simulation and through practical demonstration.

The remaining part of this paper is organized as follows. Section II introduces the air-cargo export process which is started when the cargoes arrive at the warehouse. Section III gives the spectrum measurements of the interference signals in the air-cargo warehouse. Three solutions are proposed for DRM problem in Section IV. We categorize the existing tag anti-collision Q algorithms into two groups, and then we evaluate tag anti-collision algorithms through simulation and practical item-level RFID system demonstration in Section V. Finally, we conclude in section VI.

II. Air-cargo Export Process

In this section, we summarize air-cargo movement process which is started when the cargoes arrive at warehouse as illustrated in Fig. 1. First,

* This work was supported by the IT & R&D program of SMBA, and in part by Research Collaboration among Inha University (IHU), Korea Aerospace University (KAU), General Electric (GE), and Korean Airlines (KAL) under KAGERIIC project.

* We also thanks for the work efforts of IDRO Co., Ltd.

^o Department of Electronic Engineering, Inha University (leosu8622@hotmail.com, connection83@naver.com, khchang@inha.ac.kr)

논문번호 : KICS2011-11-542, 접수일자 : 2011년 11월 22일, 최종논문접수일자 : 2011년 12월 20일

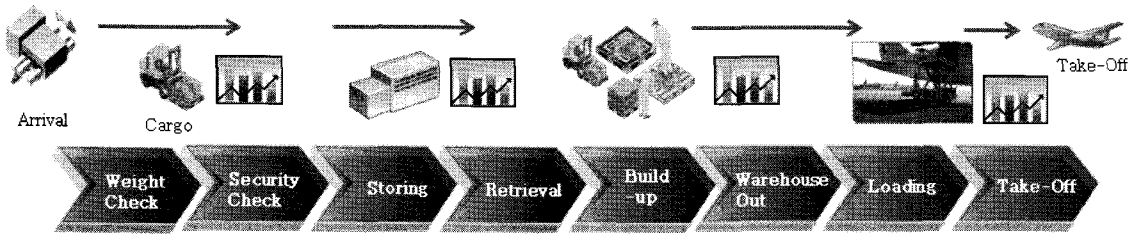


Fig. 1. Air-cargo movement process (export).

unloaded cargo is weighed, and then cargo is security checked by passing through an X-ray scanner. After that, the cargo is arranged and stored at a specific storage area according to its destination. Retrieval refers pulling out the cargo from the storage area on the timing of export. In the process of build-up, cargo is put on an ULD (unit load device) or in a container, and ULD or container number with the nested AWBs (airway bills) are recorded in the WMS (warehouse management system) server. Finally, the ULD or container gets out of the warehouse through the warehouse gate and will be loaded on an aircraft. We focus on the processes of storing, retrieval, build-up, and warehouse out in this paper.

In the process of storing, the reader implemented on the forklift can read cargo information from the tag attached on the cargo. Thus, the forklift reader can combine the AWB number and the storage area information, then send the combined information to the WMS server. In the process of retrieval, the forklift reader detaches the AWB number from the storage area information and sends the detached number to the WMS server. In the process of build-up, the handheld reader carried by staff first reads the ULD or container ID from the ULD/container tag, and then reads the AWB number of the cargo which will be nested on the ULD or container. After handheld reader matches the ULD or container ID with the AWB number, it sends the matched information to the WMS server again. Warehouse out is the process that the ULD or container gets out of the cargo warehouse through the warehouse gate. In this process, the mounted (fixed) reader, which is implemented at the warehouse gate, reads the ULD or container ID

when they pass through the gate. In this case, the mounted reader reports to the WMS server that the ULD or container has successfully got out of the warehouse.

III. Spectrum Measurement at Cargo Warehouse

In order to set up a reliable air-cargo warehouse RFID system, we do the spectrum measurement at cargo warehouse over three available RFID frequency bands, i.e. around 433MHz, 900MHz, and 2.4GHz. The measurements are taken at four zones as shown in Fig. 2, including truck dock (point A) where the cargo is unloaded from truck, transit zone (point B) where the cargo is managed to be delivered to its destination, export zone (point C) where cargo is classified and stored, and air-side zone (point D) where the ULD or container is loaded to aircraft.

For the measurement, we use the Agilent handheld spectrum analyzer (HSA) and the omni dipole antenna (ODA) which are given in Fig. 3 and Fig. 4, respectively. Fig. 5 is an example of a measurement result which is tested at truck dock in

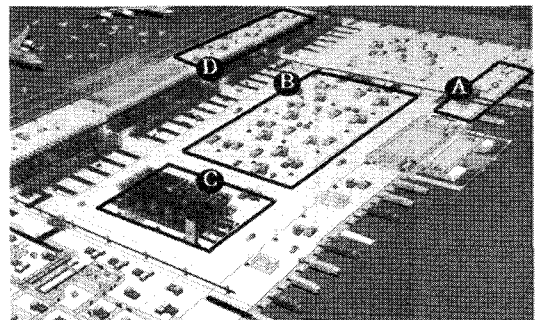


Fig.2. Spectrum test points in air-cargo warehouse.

Table 1. Interference types at four test points over three groups of RFID frequency bands.

Zone \ fc	433 MHz	900 MHz	2.4 GHz
Truck Dock (A)	<ul style="list-style-type: none"> • 322 - 328 MHz : Paging Service • 380 - 399 MHz : TRS • 440 - 450 MHz: Radiolocation (e.g. AFS) • 470 - 690 MHz : TV Broadcasting 	<ul style="list-style-type: none"> • 806 - 894 MHz : Cellular Telephone • 960 MHz - 1.215 GHz : ARN 	<ul style="list-style-type: none"> • 1.71 - 1.98 GHz : PCS • 2.40 - 2.48 GHz : ISM Band (e.g. WLAN) • 2.70 - 2.90 GHz : ARN
Transit Zone (B)	<ul style="list-style-type: none"> • 380 - 399 MHz : TRS • 420 - 430 MHz : TRS, Citizen Radio • 440 - 450 MHz : Radiolocation (e.g. AFS) • 470 - 690 MHz : TV Broadcasting 	<ul style="list-style-type: none"> • 806 - 894 MHz : Cellular Telephone • 960 MHz - 1.215 GHz : ARN 	<ul style="list-style-type: none"> • 1.71 - 1.98 GHz : PCS • 2.40 - 2.48 GHz : ISM Band (e.g. WLAN) • 2.70 - 2.90 GHz : ARN
Import Zone (C)	<ul style="list-style-type: none"> • 380 - 399 MHz : TRS • 420 - 430 MHz : TRS, Citizen Radio • 440 - 450 MHz : Radiolocation (e.g. AFS) • 470 - 690 MHz : TV Broadcasting 	<ul style="list-style-type: none"> • 806 - 894 MHz : Cellular Telephone • 960 MHz - 1.215 GHz : ARN 	<ul style="list-style-type: none"> • 1.71 - 1.98 GHz : PCS • 2.30 - 2.40 GHz : Portable Internet • 2.40 - 2.48 GHz : ISM Band (e.g. WLAN) • 2.70 - 2.90 GHz : ARN
Airside Zone (D)	<ul style="list-style-type: none"> • 380 - 399 MHz : TRS • 420 - 430 MHz : TRS, Citizen Radio • 440 - 450 MHz : Radiolocation (e.g. AFS) • 470 - 690 MHz : TV Broadcasting 	<ul style="list-style-type: none"> • 806 - 894 MHz : Cellular Telephone • 960 MHz - 1.215 GHz : ARN 	<ul style="list-style-type: none"> • 2.30 - 2.40 GHz : Portable Internet • 2.40 - 2.48 GHz : ISM Band (e.g. WLAN) • 2.70 - 2.90 GHz : ARN

TRS (Trunked Radio System), AFS (Aeronautical Freight Services), ARN (Aeronautical Radio navigation), PCS (Personal Communication Services)

433MHz frequency band. According to Fig.5, we can observe six types of interferences. They are due to the digital radio around 182.6MHz, the ARN around 230.4MHz, the paging service around 326.1MHz, the TRS around 384.8MHz, the AFS around 446.7MHz, and the TV broadcasting system around 537.0MHz. Table 1 shows all the types of frequency interference which are measured at four

test points over three groups of RFID frequency bands. The boldface in Table 1 represents the stronger interference compared to the others. Based on Table 1, we can see that most of boldface bands are belong to the aeronautical systems. However, in

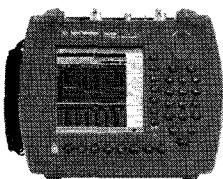


Fig. 3. Agilent handheld spectrum analyzer.

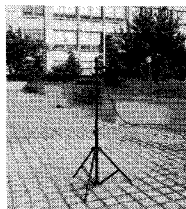


Fig. 4. Omni dipole antenna(400-460 MHz).

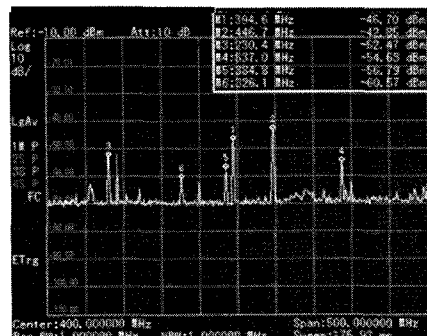


Fig. 5. Spectrum measurement of truck dock at 433 MHz band.

the place of transit zone where more staffs are gathered, the main interference comes from the service of cellular telephone.

In addition, the overall measured interference levels are given at Table 2. From Table 2, we conclude that even though there are several types of interferences existing in air-cargo warehouse, the level of interferences are not too strong to interfere an RFID system seriously. Hence, we implement the RFID system of our concern at target air-cargo warehouse.

Table 2. Interference level in air-cargo warehouse.

Zone \ fc	433 MHz	900 MHz	2.4 GHz
Truck Dock (A)	-70.07 - -54.46 dBm	-67.90 - -67.19 dBm	-65.46 - -54.37 dBm
Transit Zone (B)	-69.93 - -68.24 dBm	-68.38 - -67.51 dBm	-62.57 - -57.24 dBm
Import Zone (C)	-70.02 - -68.76 dBm	-69.47 - -66.63 dBm	-63.15 - -56.74 dBm
Airside Zone (D)	-70.01 - -69.89 dBm	-69.71 - -67.24 dBm	-64.03 - -60.95 dBm

IV. Solutions for Dense-reader Mode

In dense-readers mode (DRM)^[3], the number of simultaneously active readers is relatively more than the number of available channels (e.g. 10 active readers operating in 5 available channels). Thus, the adjacent readers often have interference on its desired signal leading the RFID system efficiency to decrease. Fig. 6 is an example of such DRM, where two readers and two tags operate under same frequency band. In Fig. 6, the reader1 gives severe interference on the reader2. This is because that the reader2 is located in the transmission range of the reader1. The RFID system throughput, however, can be improved by preventing reader interrogatory collisions via the time-division multiplexing (TDM) or frequency- division multiplexing (FDM). Fig. 7 is the DRM environment in air-cargo warehouse which includes three kinds of readers, i.e. handheld reader, forklift reader, and fixed reader. The detailed functions of those three kinds of readers are

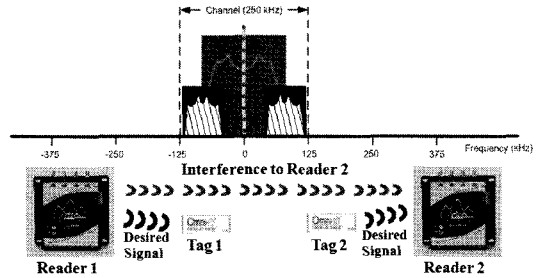


Fig.6. Example of dense-reader mode (DRM).

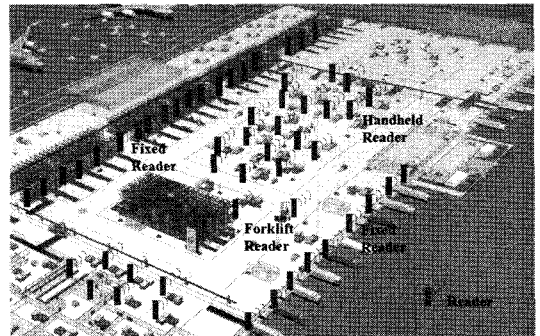


Fig.7. Dense-reader environment in air-cargo warehouse.

mentioned in section II.

In this section, we suggest three novel approaches to overcome the DRM problem in our air-cargo warehouse application. The first one is periodic transmit of a reader, which allows reader interrogating tags at a fixed time interval. This approach can be implemented into handheld readers and forklift readers in the processes of storing, retrieval, and build-up, where several forklift readers and handheld readers may operate within their adjacent reader’s transmission coverage. In order to observe the improvement by the periodic transmit strategy, we do the tests of six readers scenario where the reader antennas are distributed as shown in Fig. 8. The distance between reader antennas is 45cm, and the distance between tag to its nearest reader antenna is 34cm. We use the reader of Korean vendor IDRO, Sontec metal tag, and -2 dBi patch antenna (30*30 mm) in the following tests.

Fig. 9 is the test result of reader idle time vs. reading error rate (RER). In this test, we set the parameters as 30dBm of transmitter power, 100msec of periodic transmit time, 100msec of hopping interval, and 100,000 reading trials. According to

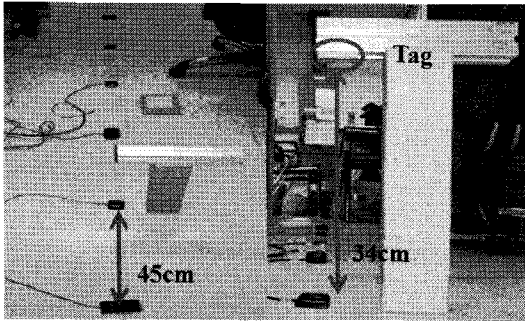


Fig. 8. Scenario of six readers and one tag

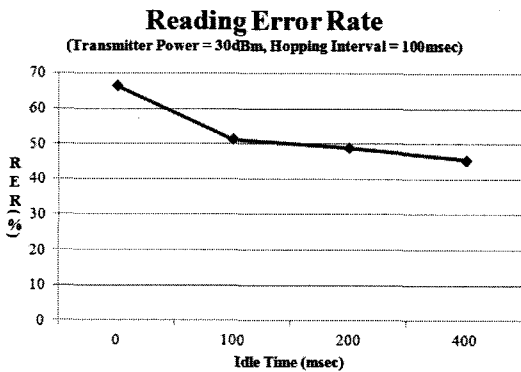


Fig. 9. Idle time vs. RER.

Fig. 9, we observe that RER is 67% with no idle time, and improved to 51% till 100msec of idle time. However, RER is only slightly improved afterwards. Second test demonstrates the performance of transmitter power vs. RER. In this test, we set the parameters as 0msec of idle time, 100msec of hopping interval, and 100,000 reading trials. Fig. 10 shows that RER has similar values over the range of transmit power 24dBm to 30 dBm. However, RER is abruptly increased by transmit power less than 24dBm. The third test is on the hopping interval vs. RER. In this test, we set the parameters as 0msec of idle time, 30dBm of transmitter power, and 100,000 reading trials. Based on Fig. 11, we can conclude that the RER is proportional to the hopping interval up to 300msec.

The second approach is using Visible RFID reader & tag as shown in Fig. 12. The RFID reader & tag based on visible light communication (VLC) are new RFID data transceiving technology for a user to designate and choose a specific tag via

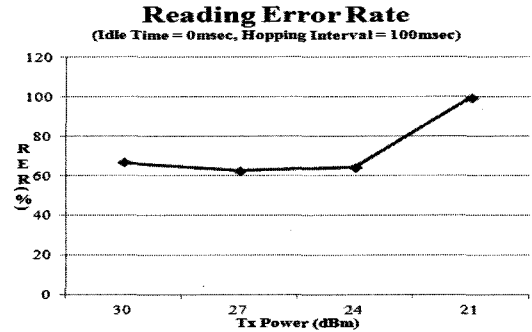


Fig. 10. Transmitter power vs. RER.

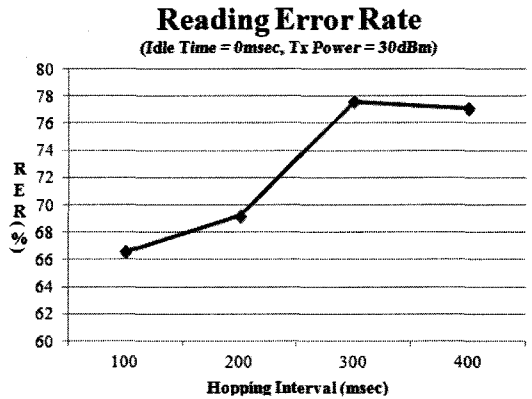


Fig. 11. Hopping interval vs. RER.

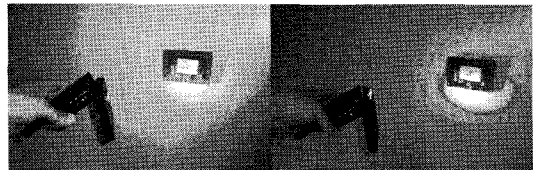


Fig. 12. Visible RFID reader and tag.

directional visible light, while conventional readers are only able to do multiple choice of tags over the area. According to the Fig. 13 of block diagrams for Visible RFID reader & tag, the reader (right side) with the protocol of 920-925MHz ISO 18000-6C^[8] interrogates the tag (left side) via VLC technology, and then the tag detects the light by using an O/E (optical to electric) transformer. On the other hand, the tag responds the reader through the RF back-scattering. The Visible RFID technology not only occupies a narrow bandwidth which can achieve effective spectrum usage but also costs low power consumption with performance improvement when SNR increases. Consequently, we can

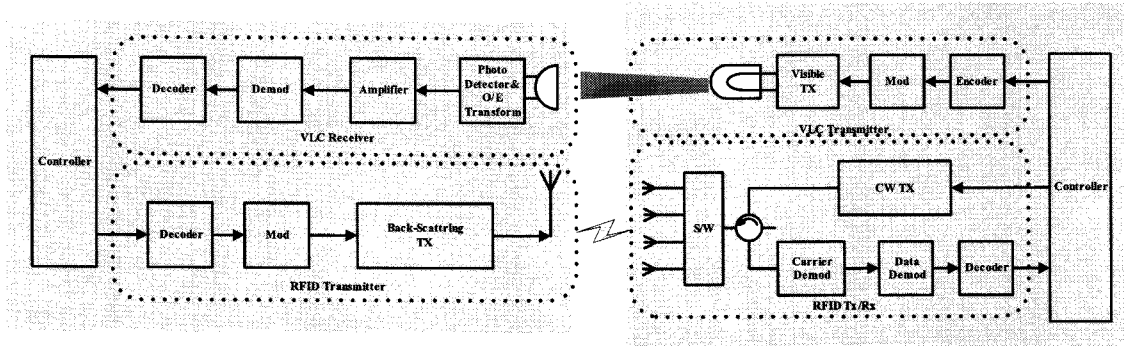


Fig.13. Functional block diagram of Visible RFID reader and tag.

implement such a Visible RFID technology into the handheld readers for the process of build-up, where the staff can use the RFID reader to interrogate target tags only, then the DRM problem can be inherently avoided. This Visible RFID technology becomes a solution for tag anti-collision also.

Another approach for the DRM problem is the sensor-based solution. In the sensor-based approach, a sensor is attached on the reader's antenna as illustrated in Fig. 14. A reader interrogates tags once the sensor detects the object. In Fig.14, the spectrum peak appears when the object is detected by sensor. The sensor-based approach can be implemented into fixed readers for air-cargo weight check and warehouse out processes. In these two processes, the

fixed readers, which are located on weighing machine and warehouse gate, interrogate the ULD/container tags only when the ULD or container passes through the weighing machine or warehouse gate.

V. Evaluation on Tag Anti-collision Schemes

In RFID system, if multiple tags respond to the reader at the same time, a tag collision occurs. An efficient tag anti-collision algorithm should decrease this collisions in order to improve the efficiency of RFID system. There are two types of tag anti-collision algorithms widely used in RFID systems. The first one is binary tree-walking scheme^[4,5]. In this scheme, if two different bit values are transmitted from the population of tags, the reader is able to detect the collision. The reader then broadcast a bit (0 or 1) indicating whether tags should continue querying. Essentially, the reader chooses a "branch" from the binary tree of ID values. Tags which do not match the reader's choice cease participating in the protocol. As the reader continues to move down the branches of the binary tree, fewer tags continue operating, and only a single tag remains at the end of the protocol. The second type is ALOHA algorithm,^{[6]-[9]} which has several versions of the algorithm. The framed slotted ALOHA (FSA) algorithm can solve the problem of high collision probability. In this scheme, time is divided into frames, and each frame consists of several slots. By adjusting the frame size, the

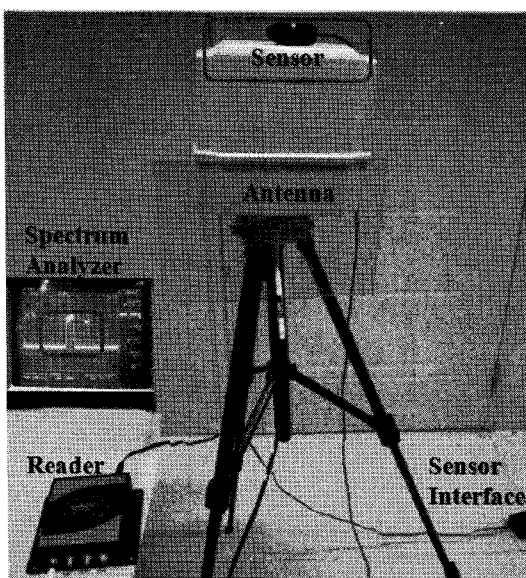


Fig.14. Configuration of sensor-based RFID system.

dynamic frame slotted ALOHA (DFSAs) algorithm can change the frame size to increase the efficiency of tag identification with the value of Q, which is an index for frame size.^[6,7] There are several variants of DFSAs Q algorithms by the way of changing Q value.^[8,9]

In this section, we divide Q algorithms into two categories. The first category is the Q algorithms which adjust frame size only when a new frame is issued with QueryAdjust command.^[8] In these algorithms, the QueryAdjust command cannot be used during a frame to modify the current frame size. We define the second category of Q algorithm named as Adjustable Framed Q (AFQ) algorithm, which implement the QueryAdjust command during a frame, and so modify the current frame size dynamically.^[9] Compared with the first category, AFQ algorithm changes the frame size multiple times during a current frame with the following criterion to decide whether the reader sends a QueryRep command or a QueryAdjust command at the beginning of the following slot. If it is not necessary to change the current frame size, the reader sends a QueryRep command. Otherwise, the reader sends QueryAdjust to modify the current frame size. Fig. 15 is the flow chart of the AFQ algorithm. The details of Q algorithms above are described as follows.

Non-AFQ Algorithm] The tag anti-collision algorithm in Gen2 is probabilistic slotted ALOHA.

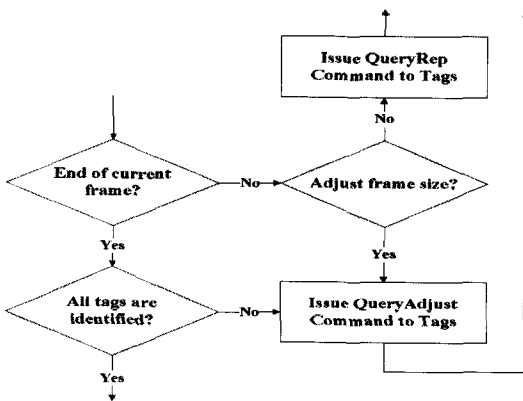


Fig.15. Flow chart of the AFQ algorithm.

It changes the frame size by varying the Q value, which is used in Query and QueryAdjust commands.^[8] Q_{fp} is a floating point representation of Q. For each slot, if a single tag replies, $Q_{fp} = Q_{fp}$. If no tag replies, $Q_{fp} = Q_{fp} - C$ due to the empty slot. When more than two tags respond the same slot, $Q_{fp} = Q_{fp} + C$ due to the collided slot. When the current frame is finished and a new Q value is required, the reader rounds Q_{fp} to the nearest integer and sets it as the value of Q. That is,

$$Q = \begin{cases} \text{round}(Q_{fp}) & \text{when single tag replies} \\ \text{round}(Q_{fp} - C) & \text{when no tag replies} \\ \text{round}(Q_{fp} + C) & \text{when multiple tags reply} \end{cases} \quad (1)$$

Here, the typical value for the constant C is chosen between 0.1 and 0.5. When Q is large, the reader uses a small value of C, and vice versa.

AFQ Algorithm] In Fixed Adjustable Framed Q (FAFQ) algorithm,^[9] in order to dynamically adjust the frame size, two threshold values are necessary to decide whether to increase or decrease the number of slots in a current frame: Th_{emp} for continuous empty slots and Th_{coll} for continuous collided slots. If the number of continuous collided slots is larger than the threshold value Th_{coll} , the current frame is finished and $Q = Q + 1$. Then, FAFQ uses a QueryAdjust command to increase the frame size, and so prevents more collisions. On the contrary, if the number of continuous empty slots exceeds the threshold value Th_{emp} , the frame size is decrease by using a QueryAdjust command to reduce the number of empty slots. Otherwise, the frame size remains unchanged. The pseudo code of FAFQ algorithm is given in Fig. 16.

In the FAFQ algorithm, the threshold values of Th_{coll} and Th_{emp} are fixed during the whole inventory procedure. If the frame size is comparably small considering the large number of tags, there will be a greater chance of slots colliding; otherwise, more chance of empty slots. Therefore, by using the variable threshold values, Adaptive Adjustable Framed Q (AAFQ) algorithm can minimize the

```

If (number of continuous collided slots) > Thcoll
    Q = Q + 1;
    Reader sends QueryAdjust;
else if (number of continuous empty slots) > Themp
    Q = Q - 1;
    Reader sends QueryAdjust;
else
    Reader sends QueryRep;
end
    
```

Fig.16. FAFQ algorithm.

frequency of transmitting QueryAdjust commands as well as minimize the identification time. It adaptively changes two threshold values for different frame sizes.^[9] The reader sends a QueryAdjust command to adjust the frame size by changing the Q value. If the value of Q is increased by 1, the frame size is doubled, which means there are too many tags, so it is necessary to increase the frame size. Accordingly, the threshold values of Th_{coll} and Th_{emp} are also increased by 1. Otherwise, they are decreased by 1. Both of them stay unchanged only if the Q is unchanged. The pseudo code of AAFQ algorithm is given in Fig. 17.

```

If (number of continuous collided slots) > Thcoll
    Q = Q + 1;
    Themp = Themp + 1;
    Thcoll = Thcoll + 1;
    Reader sends QueryAdjust;
else if (number of continuous empty slots) > Themp
    Q = Q - 1;
    Themp = Themp - 1;
    Thcoll = Thcoll - 1;
    Reader sends QueryAdjust;
else
    Reader sends QueryRep;
end
    
```

Fig.17. AAFQ algorithm.

5.1 NAFQ Algorithm

In this section, we propose a new Non-AFQ algorithm, namely NAFQ, in order to compare the performances to those of the AFQ algorithms. The general idea of this new Non-AFQ algorithm is based on the comparison of the relative frequency of empty slots (e_slots) vs. collision slots (c_slots). After the current frame is finished, if the number of e_slot exceeds the number of c_slots by a calculated threshold, the value of Q is decreased, and vice

versa. While the difference between the number of e_slots and the number of c_slots falls within the threshold, Q is unchanged.

For our proposed NAFQ algorithm, at first, we define a variable of as (2), which is an index to determine Q value. And then we vary the value of Q based on the condition in Fig.18. When the value of Q changes, or if all slots under the current Q value have been inventoried, the slot counters of the participating tag population is refreshed using a QueryAdjust command. The calculated threshold equals the current value of Q times a multiplier (set by default to 1). An inventory cycle is terminated when all slots have been checked with $Q = Q_{min}$ and no tags have been read. The whole process of Q value determination for NAFQ is described as a flow chart in Fig. 19.

```

If current frame is finished
    if (number of e_slots -  $\hat{\tau}$  * number of c_slots) > Thresh
        Q = MAX(Q-1, Qmin);
        Reader sends QueryAdjust;
    else if (number of e_slots -  $\hat{\tau}$  * number of c_slots) < Thresh
        Q = MIN(Q+1, Qmax);
        Reader sends QueryAdjust;
    else
        Q = Q;
        Reader sends QueryAdjust;
    end
    
```

Fig.18. NAFQ algorithm.

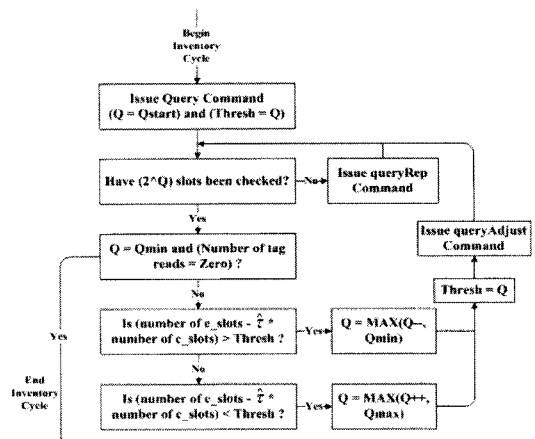


Fig.19. Flow chart of NAFQ.

$$\hat{\tau} = \frac{\text{Number of } c_slots}{\text{Number of } e_slots} \quad (2)$$

For the simulative comparison of non-AFQ and AFQ algorithms, we perform Monte-Carlo simulations for the afore-mentioned four Q algorithms, i.e., Q algorithm in Gen2, FAFQ, AAFQ and NAFQ algorithms. We compare them in term of identification time, which is defined as the time to identify all the tags in the interrogation zone. The simulation parameters are same as in [9], where both Th_{coll} and Th_{emp} are set to 10 for FAFQ. To adaptively adjust the threshold values of Th_{coll} and Th_{emp} according to the varying frame size, both Th_{coll} and Th_{emp} are set to be equal to the Q value in the AAFQ algorithm. The single responding and multiple responding tag operations are implemented in the simulation as follows.

- Single responding (SR) tag operation: In this operation, each tag is successfully identified only once. The tag disables itself when it has been identified.
- Multiple responding (MR) tag operation: In this operation, tags keep responding to the reader even if it has been successfully identified.

Fig. 20 shows the identification time of Q algorithms with the single responding tag operation. In Fig.20, NAFQ almost has the same performance as Q algorithm in Gen2. However, FAFQ and AAFQ can reduce the identification time compared to the NAFQ and Q algorithm in Gen2.

Fig. 21 describes the number of identified tags in given time interval with multiple responding tag operation, where the total number of tags is fixed at 500. According to Fig.21, AAFQ can identify the most number of tags during given time interval. The NAFQ and Q algorithm in Gen2 yield almost same performance. However, both of them are worse than AAFQ and FAFQ. According to the results of Fig.21 and Fig.22, FAFQ and AAFQ have slight performance difference when the multiple responding tag operation is implemented. But, the

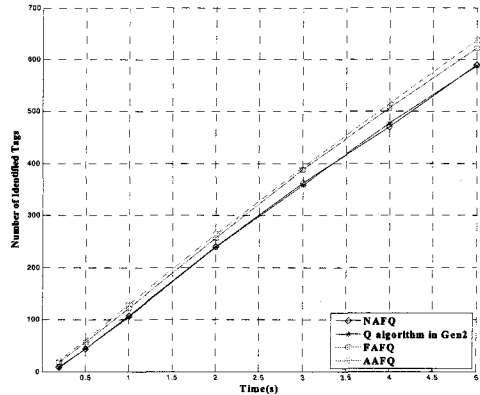


Fig.20. Identification time of Q algorithm (SR)

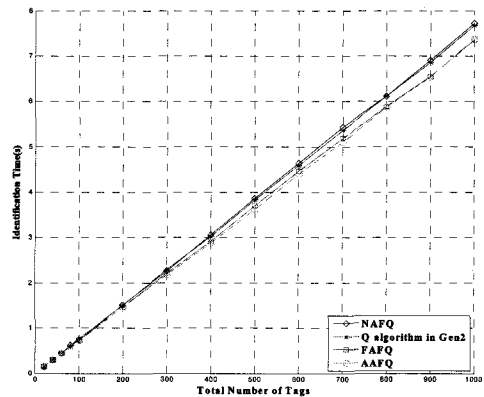


Fig.21. Nr. of identified tags by Q algorithm (MR).

performances of NAFQ and Q algorithm in Gen2 are decreased dramatically. This is mainly due to that FAFQ and AAFQ are AFQ algorithms, which can dynamically change the frame size. They only cost a small amount of time to reach the status of optimal frame size. In contrast, NAFQ and Q algorithm in Gen2 set a new frame only when the current one is finished. It inevitably spends more time to reach the status of optimal frame size.

5.2 Demonstration for Tag Anti-collision Algorithms

In our air-cargo warehouse RFID system, the proposed tag anti-collision algorithms are designed for the process of build-up. In the process, many cargo items are often kept on an ULD or in a container, and the staff uses a handheld reader to interrogate all the items correctly. However, a severe tag interrogating collision occurs, so that is why an

efficient tag anti-collision algorithm is required not only to reduce the error probability of item-level interrogatory but also to save a bulk of working hours.

To observe the performance of our proposed tag anti-collision algorithms, we implement the proposed AAFQ and NAFQ to the RFID system. The system configuration is illustrated in Fig. 22, which is composed of the Motorola reader & antenna, 100 item-level omni-ID tags, and the RFID reader controller (RRC) represented by graphic user interface (GUI). The item-level tags in Fig. 22 to be attached on cargoes are different from the ULD/container tags.

- Motorola reader and antenna: Fixed-type 2-channel Motorola reader supports Ethernet communication, and 6 dBi antenna is used for our demonstration. This antenna delivers high throughput and high capacity communication while enables organizations to capture, move and manage critical information.
- Omni-ID tags: The Omni-ID item-level tag is small enough to fit on assets with low surface area availability. With their low profile and small footprint, those tags are ideally suited for tracking and inventory control of small assets.
- RRC: It is operated in .NET environment, where it can be used in checking and managing functions of the RFID reader. The main features of RRC are shown in Fig. 23. In Fig. 23, 1

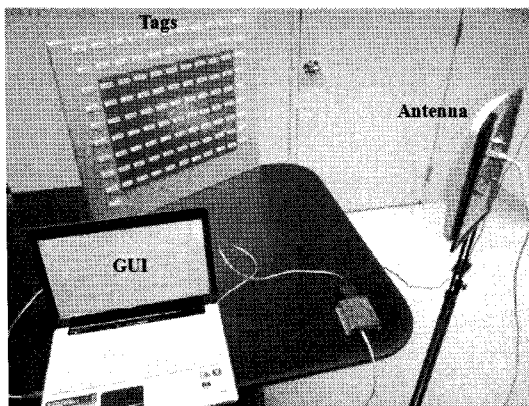


Fig.22. System configuration for tag anti-collision

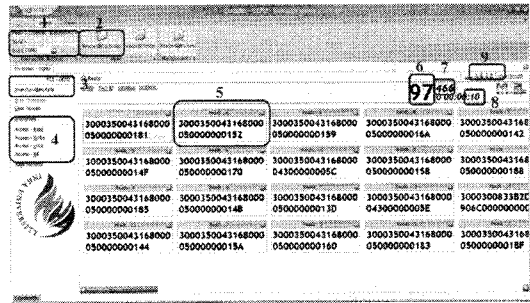


Fig.23. Main features of RFID reader controller.

represents communication port; 2: reader connection, 3: inventory execution, 4: configurations, 5: tag's ID, 6: the number of successfully identified tags among the deployed tags, 7: the number of successful reads, 8: operation time, 9: antenna selection.

For the demonstration, we use the Korean standards radio frequency band. The system power attenuation is set to 0 dBm. The radio frequency idle time and operation time are fixed as 1 msec and 80 msec, respectively. We use both session configurations of 'single responding tag operation' and 'multiple responding tag operation'. Table 3 illustrates the ensemble averages of the number of successfully identified tags among the 100 deployed tags and the number of successful reads during 10 seconds of operation time.

For 'single responding tag operation', we compare the results of the number of successfully identified tags among the 100 deployed tags (RRC: 6). According to Table.3, it shows 93 tags are identified during 10 seconds by AAFQ. However,

Table 3. Demonstration results of tag anti-collision

RRC	Single Responding Tag Operation		Multiple Responding Tag Operation	
	NAFQ	AAFQ	NAFQ	AAFQ
6	80	93	95	98
7	82	96	460	512
8	10sec	10sec	10sec	10sec
AAFQ Improvement	16.25% (Nr. of identified tags among 100 tags)		11.3% (Nr. of successful reads)	

80 tags are identified by NAFQ. The AAFQ can identify 13 tags more than NAFQ, hence leading an improvement of 16.25%.

For 'multiple responding tag operation', Table.3 shows that 98 tags, which are repetitively identified by total 512 successful reads, can be successfully identified by AAFQ within 10 seconds. 2 tags are not identified due to contention and bad channel condition. On the other hand, 95 tags are successfully identified by NAFQ, which achieves 460 successful reads. Therefore, we can conclude that AAFQ exceeds almost 11.3% of successful reads (RRC: 7) by NAFQ. In practice, we select the mode of MR, and the time to identify all the tags under MR mode is also shorter in the case of AAFQ.

VI. Conclusions

This paper aims to investigate a smart RFID system, which is used to automate the air-cargo export process, though the technologies proposed can be applied to import process also. We do the spectrum measurements compliant with the RFID frequency band at various zones in our target warehouse. The measured interference levels vary from -70 to -50 dBm that are not too strong to interfere an RFID system seriously. Furthermore, we suggest several novel solutions to overcome the DRM and tags collision problems by referring the scenarios of the cargo movement process. For the DRM problem, we give three approaches, i.e. the periodic transmit of a reader, which can improve RER to 51% till 100msec of idle time; the Visible RFID reader & tag which can designate and choose a specific tag via directional visible light; and the sensor-based RFID system which interrogates the tags once the sensor detects the object. For the tag collision issue, we categorize the existing tag anti-collision Q algorithms into two groups of non-AFQ and AFQ algorithms. According to our analysis based on the simulation and through practical demonstration, AFQ algorithms, which modify the current frame size dynamically to reach the status of optimal frame size within a very short

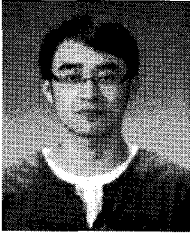
time interval, have much more desirable performances than non-AFQ algorithms in the aspects of identification time and the number of successful reads.

References

- [1] R. Want, "An introduction to RFID technology," *IEEE Pervasive Computing Magazine*, 5(1), pp.25-33, Feb., 2006.
- [2] M.M. Hossain and V.R. Prybutok, "Consumer acceptance of RFID technology: an exploratory study," *IEEE Trans. on Engineering Management*, 55(2), pp. 316-328, April, 2008.
- [3] I.C. Song, S.H. Hong, and K.H. Chang, "An improved reader anti-collision algorithm based on pulse protocol with slot occupied probability in dense reader mode" in Proc. of *VTC-spring*, pp.1-5, April, 2009.
- [4] T. Cheng and J. Li, "Analysis and simulation of RFID anti-collision algorithms," in Proc. of *Int. Conf. on Advanced Communication Technology*, pp. 697-701, Feb., 2007.
- [5] K.H. Rahman, F. Ahmed, S.A. Sagor, and Md.G. Mostafa, "An efficient anti-collision technique for radio frequency identification systems," in Proc. of *ICCIT*, pp. 1-6, Dec., 2007.
- [6] F.C. Schoute, "Dynamic frame length ALOHA," *IEEE Trans. on Communication*, 33(4), pp.565-568, April, 1983.
- [7] W. Su, N.V. Alchazidis, and T.T. Ha, "Multiple RFID tags access algorithm," *IEEE Trans. on Mobile Computing*, 9(2), pp.174-187, Feb., 2010.
- [8] EPCglobal, *Radio-frequency identity protocols class-1 generation-2 UHF protocol for communications at 860MHz - 960MHz. ver.1.1.0*, Dec., 2005.
- [9] X. Fan, I.C. Song, K.H. Chang, D.B. Shin, H.S. Lee, C.S. Pyo, and J.S. Chae, "Gen2-based tag anti-collision algorithms using chebyshev's inequality and adjustable frame size," *ETRI Journal*, 30(5), pp.653-662, Oct., 2008.

소 신 (Xin Su)

정회원



2008년 7월 중국 쿤민이공대학교 컴퓨터 공학과 (공학사)
2010년 8월 조선대학교 컴퓨터 공학과 (공학석사)
2011년~현재 인하대학교 정보통신 대학원 박사과정
<관심분야> RFID/USN Systems

장 경 희 (KyungHi Chang)

종신회원



1985년 2월 연세대학교 전자공학과 (공학사)
1987년 2월 연세대학교 전자공학과 (공학석사)
1992년 8월 Texas A&M Univ., EE Dept. (Ph.D.)
1989년~1990년 삼성종합기술원

원 주임연구원

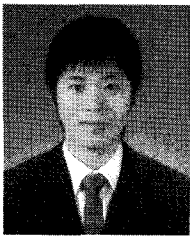
1992년~2003년 한국전자통신연구원, 이동통신연구소 무선전송방식연구팀장 (책임연구원)

2003년~현재 인하대학교 전자공학과 교수

<관심분야> 4세대 이동통신 및 3GPP LTE 무선전송방식, WMAN 및 DMB 시스템 무선전송기술, Cognitive Radio, Cross-layer Design, Cooperative Relaying System, RFID/USN Systems, Mobile Ad-hoc Network, 해상/수중 통신 등

전 광 현 (KwangHyun Jeon)

준회원



2009년 2월 강원대학교 전기전자공학과 (공학사)
2010년~현재 인하대학교 전자공학과 대학원 석사과정
<관심분야> 4세대 이동통신, Mobile Ad-hoc Network, RFID/ USN Systems